Received: 25 June 2021 | Accepted: 25 August 2021

DOI: 10.1002/pamm.202100185

On the incorporation of curvature effects into the isogeometric analysis of fibre-reinforced solids

Carina Witt[1,*], **Tobias Kaiser**[1], and **Andreas Menzel**[1,2]

[1] Institute of Mechanics, TU Dortmund University, Leonhard-Euler-Strasse 5, 44227 Dortmund, Germany
[2] Division of Solid Mechanics, Lund University, P.O. Box 118, 221 00 Lund, Sweden

In the context of engineering on the micro- and nanoscale, size-dependency is an important characteristic of material behaviour. In order to avoid complex experiments and predict size effects in simulations instead, classic continuum approaches are extended by the introduction of a length scale, e.g. through the consideration of gradient contributions. For the particular case of fibre-reinforced materials, such a gradient-enhanced approach can be achieved by introducing the fibre curvature as an additional kinematic quantity. This implies that basis functions with a global continuity higher than C^0 are required for a finite element-based approach which accounts for these fibre curvature effects. The present contribution shows that the isogeometric finite element method can provide a framework for the simulation of the respective higher-gradient continua.

1 Constitutive model with fibre curvature contributions

Based on the derivations in [1], a general form of the stored energy density $W(I_i(\boldsymbol{\varepsilon}, \boldsymbol{a}_0, \boldsymbol{\gamma}))$ is proposed for fibre-reinforced materials. In particular, the $\mathrm{n_I}$ invariants I_i depend on the first and second gradient of the displacement field $\boldsymbol{u}$ through the kinematic quantities

$$\boldsymbol{\varepsilon} = \nabla_{\boldsymbol{x}}^{\mathrm{sym}} \boldsymbol{u} \quad \text{and} \quad \boldsymbol{\gamma} = \nabla_{\boldsymbol{x}} \boldsymbol{a}_t = [\nabla_{\boldsymbol{x}} \nabla_{\boldsymbol{x}} \boldsymbol{u}] \cdot \boldsymbol{a}_0. \tag{1}$$

They represent the small strain tensor as well as the gradient of the deformed fibre vector field $\boldsymbol{a}_t$ under the assumption of initially straight fibres. In [1], it is further proposed to only consider the projection of $\boldsymbol{\gamma}$ onto the initial fibre direction $\boldsymbol{a}_0$ in the energy function. Accordingly, a quadratic form of the corresponding energy term would, e.g., read

$$W^{\boldsymbol{\gamma}} = c\, I_6, \quad I_6 = [\boldsymbol{\gamma} \cdot \boldsymbol{a}_0] \cdot [\boldsymbol{\gamma} \cdot \boldsymbol{a}_0] \tag{2}$$

with the scalar parameter c accounting for the fibre bending stiffness, see [2] and references cited therein.
The consideration of this higher gradient energy contribution leads to an, in general, non-symmetric stress tensor which is characteristic for the couple-stress theory, cf. [3]. Consequently, differentiation of the stored energy density function with respect to the strain tensor only provides the symmetric part of the stress tensor, whereas the deviatoric part of the so-called couple-stress tensor $\boldsymbol{m}$ is additionally obtained from the derivative with respect to the higher-gradient term $\boldsymbol{\gamma}$, i.e.

$$\boldsymbol{\sigma}^{\mathrm{sym}} = \sum_{i=1}^{\mathrm{n_I}} \frac{\partial W}{\partial I_i} \frac{\partial I_i}{\partial \boldsymbol{\varepsilon}}, \quad \left[\boldsymbol{m}^{\mathrm{dev}}\right]^{\mathrm{t}} = \frac{2}{3}\, \boldsymbol{\epsilon} : \sum_{i=1}^{\mathrm{n_I}} \frac{\partial W}{\partial I_i} \left[\boldsymbol{a}_t \otimes \frac{\partial I_i}{\partial \boldsymbol{\gamma}} + \left[\frac{\partial I_i}{\partial \boldsymbol{\gamma}}\right]^{\mathrm{t}} \otimes \boldsymbol{a}_t \right], \tag{3}$$

cf. [1]. The skew-symmetric stresses, on the other hand, are a direct consequence of the balance of angular momentum as briefly discussed in Section 2. The spherical counterpart of the couple-stress tensor remains indeterminate, cf. [3].

2 Higher-gradient continua and isogeometric finite element approach

The isogeometric finite element approach to higher-gradient continua which can account for curvature effects in fibre-reinforced solids is based on the balance equations of linear and angular momentum derived from the couple-stress theory, cf. [3],

$$\nabla_{\boldsymbol{x}} \cdot \boldsymbol{\sigma}^{\mathrm{t}} + \rho\, \boldsymbol{b} = \rho\, \dot{\boldsymbol{v}}, \tag{4}$$

$$\nabla_{\boldsymbol{x}} \cdot \boldsymbol{m}^{\mathrm{t}} + \rho\, \boldsymbol{c} - 2\, \mathrm{axl}(\boldsymbol{\sigma}) = \boldsymbol{0}. \tag{5}$$

Therein, ρ denotes the mass density, $\dot{\boldsymbol{v}}$ is the time derivative of the velocity field, and volume-distributed forces and couples are represented by $\boldsymbol{b}$ and $\boldsymbol{c}$, respectively. From (5), the skew-symmetric part of the stress tensor can be deduced so that, with (3) at hand, the tensor $\boldsymbol{\sigma} = \boldsymbol{\sigma}^{\mathrm{sym}} + \boldsymbol{\sigma}^{\mathrm{skw}}$ is fully described. By neglecting the volume-distributed forces and couples, the insertion of (5) into (4) leads to a 4th-order partial differential equation

$$\nabla_{\boldsymbol{x}} \cdot \boldsymbol{\sigma}^{\mathrm{sym}} + \frac{1}{2}\, \nabla_{\boldsymbol{x}} \times \left[\nabla_{\boldsymbol{x}} \cdot \boldsymbol{m}^{\mathrm{t}}\right] = \rho\, \dot{\boldsymbol{v}} \tag{6}$$

* Corresponding author: e-mail carina.witt@tu-dortmund.de, phone +49 231 755 5737, fax +49 231 755 2688

in which the 4th-order gradient term results from the divergence of the skew-symmetric stress contributions. With test function $\boldsymbol{\eta}$, the weak formulation of the internal contribution

$$\mathcal{W}_{\text{int}} = \int_{\mathcal{B}} \nabla_{\boldsymbol{x}} \boldsymbol{\eta} : \boldsymbol{\sigma}^{\text{sym}} \, \mathrm{d}v + \int_{\mathcal{B}} \left[\nabla_{\boldsymbol{x}} \left[\frac{1}{2} \nabla_{\boldsymbol{x}} \times \boldsymbol{\eta} \right] \right] : \boldsymbol{m}^{\text{t}} \, \mathrm{d}v \tag{7}$$

shows the resulting higher continuity requirements due to the product of higher-order gradients in the integrals. Within the proposed isogeometric finite element framework, Non-uniform Rational B-Splines basis functions R of degree p are used for the discretisation of (7). They can be shown to be C^{p-1}-continuous across element boundaries, see [4], so that the required global continuity can be achieved. The internal force vector for an element e accordingly results in

$$\boldsymbol{f}^{e}_{\text{int}} = \sum_{A=1}^{\text{n}_{\text{en}}} \int_{\mathcal{B}^e} \nabla_{\boldsymbol{x}} R^A \cdot \boldsymbol{\sigma}^{\text{sym}} \, \mathrm{d}v + \int_{\mathcal{B}^e} \left[\frac{1}{2} \boldsymbol{\epsilon} \cdot \nabla^2_{\boldsymbol{x}} R^A \right] : \boldsymbol{m}^{\text{t}} \, \mathrm{d}v \tag{8}$$

with n_{en} denoting the number of active basis functions on the element and with the permutation symbol $\boldsymbol{\epsilon}$ which, together with the second gradient of the basis functions, results from the curl operator in (7).

3 Representative boundary value problem

A fibre-reinforced cantilever beam under a bending deformation is analysed with the proposed isogeometric framework, making use of a globally C^1-continous approximation of the displacement field. The fibres are aligned with the beam's axis and are assumed to exhibit a bending stiffness so that fibre curvature effects are accounted for. Fig. 1-3 show that the proposed method is capable of reproducing size effects that occur as a consequence of variable fibre bending stiffness values or different geometric dimensions. Beams with a different height-to-length (h/l) -ratio have been simulated subject to a prescribed vertical force F at the tip of the beam. In accordance with the Bernoulli beam theory, the force has been scaled cubic in comparison to the scaling factor of the height so that the analytically calculated maximum displacement $u_{\max} = F\, l^3/[3\, E\, I_y]$ with length $l = 150\,\text{mm}$ and area moment of inertia $I_y \sim h^3$ remains constant independently of the slenderness. For the Young's modulus $E^* = 1.2000 \times 10^5$ of the material, the correction $E = E^*/[1-\nu^2]$ with $\nu = 0.35$ is used in order to account for the plane strain state in the simulations. Fig. 1 shows that for a vanishing fibre bending stiffness, the deflection of the beam is hardly affected by its slenderness. A small deviation from the analytically obtained constant value, however, can be observed in Fig. 3. This is due to the increasing discrepancy with the assumption of slim beams when the h/l-ratio takes high values. If the fibre curvature effect is activated by setting $c > 0$, a stiffer response is observed, see Fig. 2 and 3. This effect is most prominent for slim beams, as revealed in Fig. 3.

For further investigations of the influence of the fibre bending stiffness, the interested reader is referred to [2] and [5] where additional boundary value problems are analysed, including a comparison with an analytical solution for an isogeometric finite element framework with consideration of small as well as finite strains.

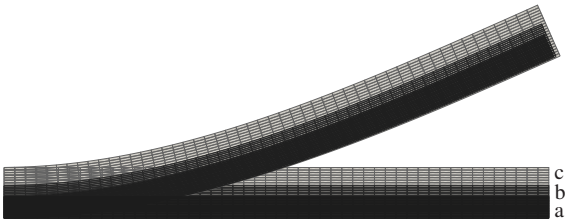

Fig. 1: Initial and deformed configuration of a fibre-reinforced beam with $c = 0$ and $h/l \in \{$(a) 0.04,(b) 0.06,(c) 0.08$\}$.

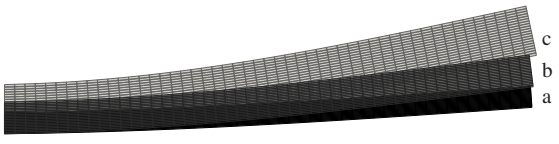

Fig. 2: Deformed configuration of a fibre-reinforced beam with $c = 10^6$ N and $h/l \in \{$(a) 0.04,(b) 0.06,(c) 0.08$\}$.

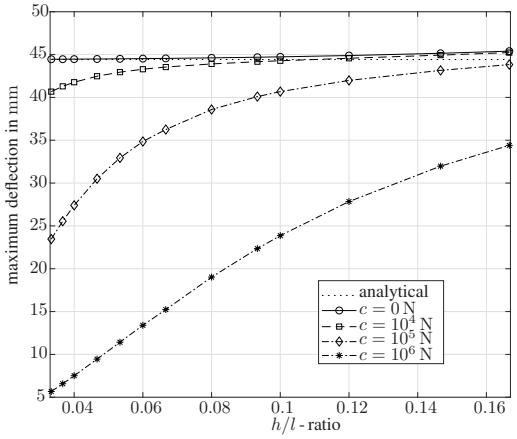

Fig. 3: Maximum deflection of a fibre-reinforced beam in dependence of its slenderness h/l and fibre bending stiffness c.

Acknowledgements Open access funding enabled and organized by Projekt DEAL.

References

[1] A. J. M. Spencer, K. P. Soldatos, Int. J. Nonlinear Mech. **42(2)**, 355-368 (2007).

[2] C. Witt, T. Kaiser, and A. Menzel, Arch. Appl. Mech. **128(15)**, (2021).
[3] R. D. Mindlin, H. F. Tiersten, Arch. Ration. Mech. Anal. **11(1)**, 415-448 (1962).
[4] J. A. Cottrell, T. J. R. Hughes, Y. Bazilevs, Isogeometric Analysis: Toward Integration of CAD and FEA (Wiley a John Wiley and Sons Ltd. Publication, Chichester, 2009).
[5] C. Witt, T. Kaiser, and A. Menzel, J. Eng. Math. **91(2)**, 643-672 (2021).